Algerian Journal of Engineering and Technology

Journal homepage: https://jetjournal.org/index.php/ajet

Original Article

Phase formation and structure in rapidly quenched $Ni_{50}Al_{50}$ alloy

Youcef Khenioui[a]*, Djaffar Saidi [a], Bachir Zaid [a], Mohamed Sadouki [a], Nassim Souami [b], Badis Rahal [b].

[a] *Department of Structural and Cladding Materials, Division of Fuel Technology, Draria Nuclear Research Center, Algiers, Algeria*
[b] *Department of material Physics, Division of physics, Algiers Nuclear Research Center, Algiers, Algeria*

ARTICLE INFO

Article history:
Received 02 October 2023
Revised 22 October 2023
Accepted 30 October 2023

Keywords:
SEM;
XRD;
NiAl,
Alloy,
Nanoparticles.

ABSTRACT

A novel synthesis process combining arc melting and rapid quenched system has been developed to manufacture $Ni_{50}Al_{50}$ alloy which is not easy to form using conventional fabrication approaches. In this work, Nickel-Aluminum alloys with nominal composition Ni50at%Al50at% were prepared by melting pure nickel pieces (99.97%) and pure Al pieces (99.999%) under the protection of argon atmosphere using induction furnace followed by experiments performed by a new in-situ solidification method with arc melting. Alloy so produced is characterized by a compact structure with a minimum porosity. X-ray phase analysis revealed the existence of a one-phase structure of the rapidly quenched $Ni_{50}Al_{50}$ alloy. In this study, rapid quenching in liquid nitrogen from a high-temperature (1638 °C) state resulted in a non-uniform grain size distribution for $Ni_{50}Al_{50}$ alloy. Some grains were as small as 20 nm, while larger grains reached about 100 nm, with an average diameter of 74.8 nm. In contrast, cast ingots made with an induction furnace had larger average grain sizes (160-600 nm). These findings demonstrate the potential to create nanocrystalline structures in the $Ni_{50}Al_{50}$ alloy through rapid solidification in liquid nitrogen, offering the possibility of milling the synthesized alloy into nano-powders for composite matrix use during sintering. The nano-structuration behaviors and microstructures for $Ni_{50}Al_{50}$ alloy synthesis and powders nanoparticles obtained by milling have been investigated with the aids of Optical Microscopy (OM), X- Ray Diffraction (XRD) and Scanning Electron Microscopy (SEM).The results show that the samples rapidly quenched in liquid nitrogen from high temperature as solidus state with temperature slightly lower than 1638°C, restrain the precipitation of NiAl phase as clusters, consequently, the NiAl specimens above solidus follow by rapidly quenched in liquid nitrogen among NiAl nanoparticles make the phase distributes homogeneously.

1. Introduction

NiAl alloy has a relatively wide single phase field with composition between 45-60 at % Ni, with CsCl crystal structure (B2) which has a high melting point (1638°C) with many advantages such as low density (5.91 g/cm3), high thermal conductivity, (75 W/mK) and excellent oxidation resistance in its completely ordered state [1,7]. Because of these properties, NiAl is a material of technological interest with several potential engineering applications as corrosion-resistant coatings [7-11]. It has also replaced Ni-based super alloys for the manufacturing of high-temperature turbine blades and vanes

A research and development efforts on aluminium alloys using techniques such as rapid solidification have focused attention on the prospects for the creation of new engineering alloys. The properties achievable through rapid solidification improve the behaviour of the synthesis alloys but also developing novel alloy composition.

*Corresponding author.
E-mail address: y-khenioui@crnd.dz
Peer review under responsibility of University of El Oued.
 https://dx.doi.org/10.57056/ajet.v8i2.127

Rapid quenching of melted metals and alloys has been recognized as a process for obtaining nanosized particles [12]. The driving force for nanostructuration is connected to the degree of supercooling gradient (ΔT) [12-14]. Subsequent nanostructuration of the obtained material (with mixed amorphous and crystallized phases) allows the formation of nanopowders. When we deal with rapid quenched alloys, preferential refined particles intervenes [15] and is furthermore expected enhancement of the reactivity induced the high specific area of the surfaces. This idea could provide means for obtaining nanosized particles through a particular top-down synthesized mode. It is the purpose of this work to point out the prospect of such a process. The best way to reveal this potential process is to select an alloy with a high demixtion capacity.

In the NiAl system, there exist several intermetallic compounds [diagram], namely, NiAl3, Ni2Al3, NiAl, and Ni3Al. Among these alloys, NiAl and Ni3Al are known to be promising high-temperature structural materials owing to their excellent strength at high temperatures and oxidation resistance [3,4].

In this work, we consider $Ni_{50}Al_{50}$ alloy. Such a composition makes possible the formation of intermetallics during the cooling process [16]. Incidentally, these intermetallics are of interest as they provide also means for hydrogen trapping via hydruration reactions [17-18].

Also, nanoparticles and nanopowders materials have been largely used in industrial and technological applications. The results of nanotechnology from the recent research are largely integrated in the industrial processes necessary for the manufacture and the development of a large variety of products used in the everyday life application as:

-In chemistry due to higher surface area reactivity and good for heterogeneous catalysis with high level of reaction control

-In mechanics due to his better mechanical strength

-In physics due to the quantum confined phenomena and designed physical properties as magnetic storage and plasmonics.

Besides that, the self-organization of nanoparticles (NPs) is another major area of research since it has many practical applications [18]. Because of their special size, a large number of particles are present at the surface compared to that of the bulk. For this reason, nanostructured materials have found potential utility in a wide range of catalytic and gas sensing, applications [19,20].

During these last decades, several techniques of development were implemented to manufacture nanopowders [21]. Among these techniques one can quote particularly those having applications in the field of hydrogen storage [17]. The nanoparticules were synthesized by means of a large variety of techniques such as the treatment ground-freezing [22,23], the mechanical alloying [24], by the melt-spenning [25], the synthesis by plasma [26], rapid solidification [27,28], the synthesis by combustion [29], the hydrothermal synthesis by ultrasounds [30] and laser ablation [31].

The top down method is a promising method for the synthesis of the nanoparticules as $Ni_{50}Al_{50}$ due to its simplicity and its low temperatures of reaction [14]. Thus, the nanoparticles NiAl synthesized by this technique makes it possible to lead to the manufacture a solid material by sintering method.

The current work investigates the in situ processing of nanostructured intermetallic $Ni_{50}Al_{50}$. This paper is focused on obtaining nanopowders with the use of a new technique. The alloy is first processed by using induction furnace followed by a laboratory arc melting furnace and then rapidly quenched the samples to the liquid nitrogen. It should be noted that the essential difficulty in this technique depends in the agglomeration and the growth of the nanoparticles which in addition was the subject of several research tasks [12].

Therefore, effects of the phase transformations during the process may be of prime importance to the densification process, as well as to the final phase of the nanopowders synthesis. The phase content has a considerable impact on the final properties of nanopowders structure [14]. The substructures of the as-solidified by ultra-rapid quenched alloys were examined.

Also, the motivation for the current work on the nanostructured $Ni_{50}Al_{50}$ is the grain size refinement [2] as a new method for improving properties of conventional materials synthesized by sintering method. The real challenge is to develop an alloy which has the required phase microstructure (β-NiAl) and facilitates the production of the nano-grains by means of mechanical milling. This alloy was studied in as-cast and with rapidly quenched conditions. Therefore, the aim of this work was to develop a new process for the synthesis of $Ni_{50}Al_{50}$ and studied the influence of the samples as-unquenched and as-rapidly quenched samples on the morphology and describes the microstructures of $Ni_{50}Al_{50}$ synthesis and nano powder obtained by mean of this new process.

2. Materials and Methods

2.1. Ni-Al Alloy Synthesis

$Ni_{50}Al_{50}$ melts congruently at 1638°C and has a wide single phase field which extends from 45 to 60 at.% Ni. The ordered beta B2 (CsCl prototype) crystal structure of NiAl consists of two interpenetrating primitive cubic cells, where Al atoms occupy the cube comers of one sublattice and Ni atoms occupy the cube corners of the second sublattice. In this study, Two-step method of synthesizing bulk nanostructured $Ni_{50}Al_{50}$ alloy was used. One-step methods consist of synthesizing bulk $Ni_{50}Al_{50}$ alloy by induction melting pure elements which is of pure elements (purities of 99.99% for Aluminum and 99.97% nickel respectively) the composition is nominally expressed in atomic per cent under argon atmosphere. The laboratory ingot was performed in Leybold furnace type of intermediate frequency (MF IS 01). Afterwards, the obtained ingot was cut and subdivided into little samples of 20.0 g. In the step two, the ingot obtained by induction furnace was re-melted three times to ensure good homogeneity by arc melting under pure argon atmosphere (5 ingots were prepared). After that, the melt of $Ni_{50}Al_{50}$ alloy in the ultimo liquidus phase, was rapidly ejected out from the copper mould and dropped into liquid nitrogen temperature. Consequently, the sample in final step is fabricated by as rapid in-situ solidification. This new rapid quenched processing device was designed and realized in our laboratory with good performances already tested in our previous study. A detailed description of the experimental procedures used in the process (step two) has been reported in our previous work [32].

2.2. XRD Characterization

The X'pert Pro diffractometer of Philips was recorded to identify the crystalline structure of NiAl alloy and powder using a copper X-Ray tube (λcu = 0.154059 nm) with a generator voltage of 45 Kv and X-Ray tube current fixed to 40 mA, for diffraction angle ranging between 20 and 100◦. The Scanning Electron Microscopy (SEM) and transmission electron microscopy (TEM) characterization was performed to study size and shape particle using respectively Philips environmental microscope (FEI/Philips XL30 FEG ESEM) coupled with an energy dispersion spectroscopy analyzer (EDS) and Jeol, transmission electron microscope (model JEOL JEM-2010) operated at 200 kV with an optical point to point resolution of 0.23 nm. The sample was dispersed in ethanol prior to the TEM measurement. The as-solidified microstructures were revealed by etching the polished specimens with a mixture of nitric acid water solution (5%HF+45 ml HNO_3+50 ml H_2O).

3. Results and discussions

3.1 Optical and SEM Analysis

In order to understand the microstructure evolution of NiAl alloy during rapidly solidification, the samples were examined by using optical microscope (OM) and secondary electron microscopy (SEM).

3.1.1 Optical analysis

The microstructure of the alloy as synthesized by induction furnace is shown Fig.1. We can clearly see a columnar grain growth in $Ni_{50}Al_{50}$ alloy. In the second step, rapid solidification experiments were carried out, including arc melting furnace equipped by a new system consisting of rapid quenched materials conceited and realized in our laboratory. The morphology of $Ni_{50}Al_{50}$ alloy as achieved and fabricated by arc melting followed by ultrarapid solidification is show in Fig.2. In this step, optical microscopy showed typical fine grains growth and dendritic structure in the as rapid solidified specimen of $Ni_{50}Al_{50}$ alloy. In Fig.2a, we can see colonies of primary and secondary dendrites beside the fine grains. Furthermore, in some zones martensite lath packs with different streaks laths orientations and sizes are observed in Fig.2b in agrement with literature [37]. Globally the morphology presents a pronounced isotropic grain structure Fig.3.

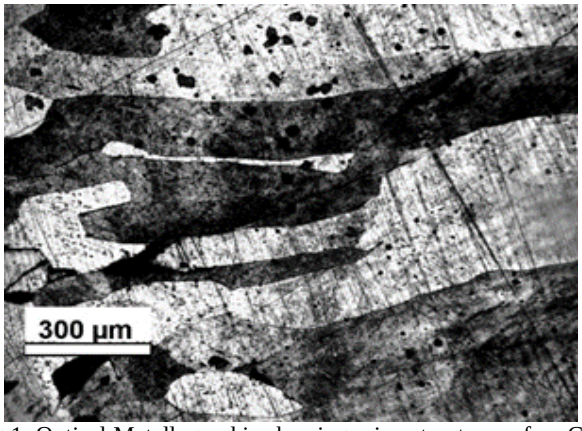

Fig 1. Optical Metallographic showing microstructures of as-Cast Ni50Al50 alloy synthesized with induction furnace showing a columnar grains.

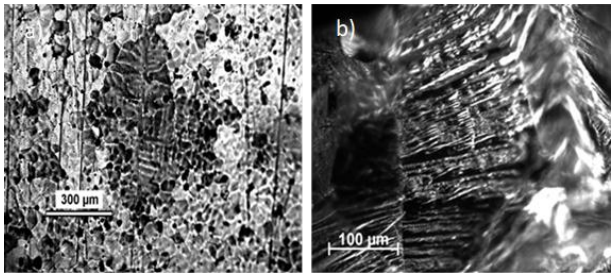

Fig 2. The optical micrograph of the microstructure of the rapidly quenched Ni50Al50 alloy. a) overview of the cooling dendritic structure. b) zone indicated the presence of a colony of platelets.

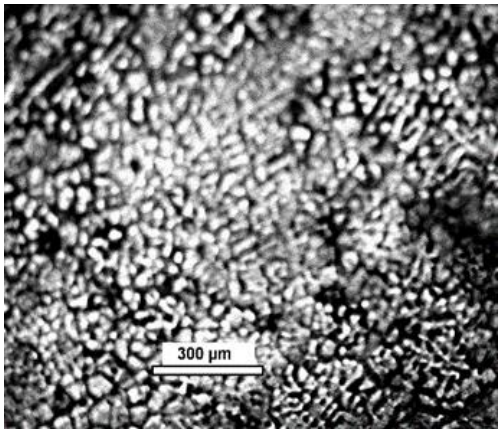

Fig 3. The optical micrograph of the microstructure of the rapidly quenched Ni50Al50 alloy.

Fig 3. Shows the typical optical micrograph of the microstructure of the rapidly quenched $Ni_{50}Al_{50}$ alloy. The results of the microstructures are the uniform and fine dispersion of crystallites.

3.1.2 SEM Observation

The rapid solidification of $Ni_{50}Al_{50}$ alloy under high gradient temperature of the solidus dropped rapidly to the liquid nitrogen makes the primary dendrite skeleton disintegrate into refined grains sizes Fig.4.

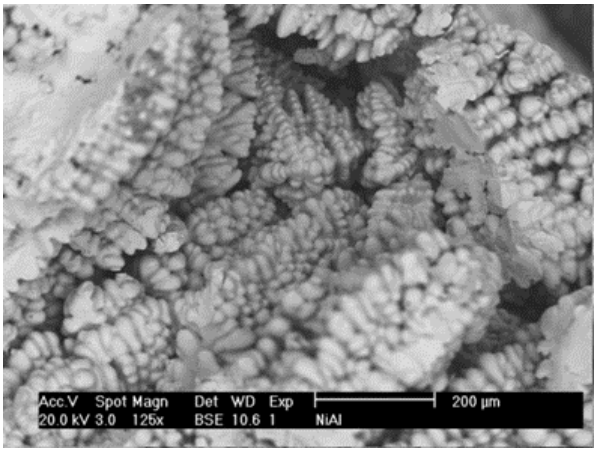

Fig 4. SEM/BSE image showing the morphology of rapidly quenched Ni50Al50 alloy from solidus temperature (less than 1638°C) to liquid nitrogen.

Consequently, as seen at great magnification, dendritic crystal disappears from grain refined morphologies under sufficiently undercooled conditions, in agreement with others literature results [33,34]. Globally, the SEM observations of quenched surface samples reveal a dendrite state as shown in Fig.4 in chemically etched region after mechanical polishing. A dendrite structure characterized by a main branch, made of nano-scaled particles, to which are attached series of secondary branches as also reported by B. Wei [14]. The open porosity interdendrite shows in Fig.5 are quite important, which in conjunction with the nanosized nature of the particles, allows high reactivity of the material.

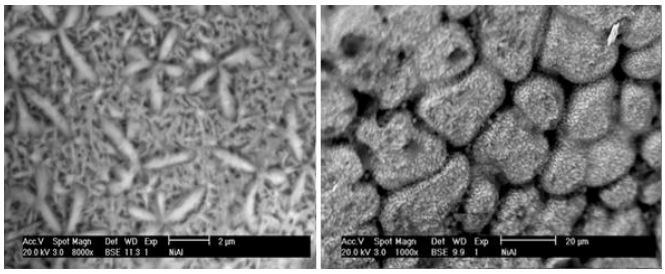

Fig 5. SEM/BSE micrographs of rapidly quenched Ni50Al50 alloy.

The size, shape and agglomeration behavior of $Ni_{50}Al_{50}$ nanoparticles was observed using high magnification by scanning electron microscopy (SEM). Fig.6, show the microstructural SEM as backscattered (BSE) images of the NiAl alloy as synthesizes by arc melting followed by ultra rapid solidification mode. The particles size was found to be nearly semi spherical and naturally agglomerate. Also, From the BSE images results, the small crystallites were found approximately equal to 74.8 nm Fig 6b. Enhancement of magnification of unquenched material, Fig.6a, shows that the grain size of $Ni_{50}Al_{50}$ alloy is not uniform, some fine grains are smaller than 160 nm, and the bigger grains are about 600 nm.

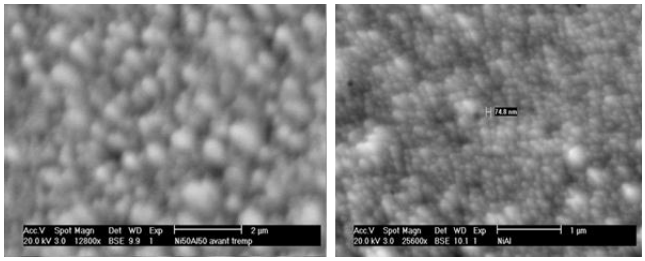

Fig 6. SEM-micrographs of Ni50Al50 alloy a) Sample Before rapidly quenching: Revealing the nanostructure of the grains and exhibiting semi-spherical grains with diameters ranging from approximately 160-600 nm.
b) Sample After Rapidly Quenching in liquid nitrogen: Highlighting the occurrence of cluster agglomeration and displaying semi-spherical grains with an average diameter of approximately 74.8 nm.

3.1.3. XRD Analysis

The crystalline structure was analyzed by X-ray diffraction (XRD) using X'Pert Pro of Philips diffractometer (X-ray tube Cu: λ = 1.54059 Å and generator settings: 45 Kv, 40 mA).The interesting query of the nature of the phases is investigated by XRD and the results are shown in Fig.7. The Nickel - Aluminum phase diagram [1], show a rich one and includes five different compositions. Most of these compositions are not stoichiometric, Al3Ni, Al3Ni2, AlNi, Al3Ni5 and AlNi3. X-ray analysis revealed the existence of one phase structure (beta-NiAl). The diffraction peaks of the nanostructured $Ni_{50}Al_{50}$ alloy well with the diffraction

data from the JCPDS card No. 03-065-0420. The peaks Intensity (a.u) at 2 Theta (deg) at values of 30.9, 44.33, 55, 64.50, 73.25, 81.62, 98, 115 correspond to the (100), (110), (111), (200), (21 0), (211), (220) and (310) respectively, which could be readily assigned to a cubic phase of $Ni_{50}Al_{50}$ with a B2-ordered crystal structure (CsCl prototype) which is retained up to the melting temperature of about 1911 K [35]. The structure of NiAl is B2, which consists of nickel atoms at the cube corners and a single aluminum atom at the body centered position.

No characteristic peak related to any other impurity was observed. Further, our observation revealed that the samples $Ni_{50}Al_{50}$ alloy had sharp peaks, which indicated a good crystallinity. From the XRD results (Fig.7) for $Ni_{50}Al_{50}$ alloys it is found that the rapid quenching approach shown depresses of the formation Al and Ni secondary's phases, implying a more homogeneous distribution of Al and Ni in the $Ni_{50}Al_{50}$ alloy. In addition, no impurity phases are detected; indicating that rapidly quenched samples in liquid nitrogen does not destroy the structure of $Ni_{50}Al_{50}$ alloy.

In addition, for un-quenched sample, it reveals that the relative slow cooling rate results in the formation of tree phases with different nickel contents identified by XRD as respectively NiAl, N3Al and Ni0.58Al0.42 crystalline structures Fig.7a. The lattice parameters of the structures are shown in Table 1. Compared with the rapidly quenched one, the unit cell is slightly contracted along directions for NiAl, Al0.42Ni0.58 and Expended for Ni3Al. The higher relative density observed in the unquenched $Ni_{50}Al_{50}$ alloy, as indicated in Table 1, is attributed to the lower presence of porosity. Quensequently the increased density can be attributed to the absence of liquid nitrogen quenching.

The average crystallite size of the particles and the lattice parameters for $Ni_{50}Al_{50}$ composition are also determined from the width of the XRD line using Scherrer's formula.

The crystallite size of rapidly quenched and unquenched samples was estimated using Scherer's formula [36]. The mean crystallite dimensions of as synthesized NiAl alloy before and after rapidly quenched can be calculated from the width of the profiles of the nickel-Aluminum reflections according to the classical Scherrer relation: $L = K\lambda/\beta\cos\theta$ where L is the size of crystallite in Å, λ the X-ray wavelength in Å, K the constant with the value of 0.9, θ the Bragg angle for the reflection and β is the observed peak width at half maximum intensity for the results are summarized in Table 1. The as-quenched material was found to consist of predominantly the β-NiAl phase indicating that the cooling rate during melt solidification was rapid enough to suppress totally the diffusional decomposition of β-NiAl. In the unquenched material as seen in Fig. 7a, the formation of tree phase partially in β-NiAl phase has been observed and this structure can be obtained from the high-temperature β phase with the type structure to partial expensed cubic transformation of B2-NiAl to tree cubic-NiAl structure [38]. The presence of tree phases in the unquenched alloy is due to the formation of nickel enrichment phases. The average crystallite size was estimated to around respectively 62 nm and 160-600 nm respectively for the sample rapidly quenched in liquid nitrogen and unquenched one. Our findings are in good agreement with recent experimental.

Table 1: XRD lattices parameters, densities and average crystallites sizes obtained by respectively SEM image and Scherer's equation.

NiAl Alloy Composition (At%)	Phase of the nanoparticles	XRD Lattice parameter (Å)	Average crystalline size calculed by SEM (nm)	Average crystalline size calculed by XRD (nm)	Density g/cm3
$Ni_{50}Al_{50}$ after rapid solidification	NiAl Cubic	2,8870(8) In agreement with JCPDS code 03-065-0420	74	66	5.9 close to the value given by Y. Sun et al [39]
And another entry	NiAl Cubic	2.875(3) In agreement with JCPDS code 03-065-0420	160-600	140	5.91 close to the value given by O. Ozdemir et al [40]
$Ni_{50}Al_{50}$ before rapid solidification	Al0.42Ni0.58 Cubic	2.871 In agreement with JCPDS code 00-044-1267			6.3 close to the value given by Povarova et al [41]
	AlNi3 Cubic	3.553 In agreement with JCPDS code 03-065-0430			7.51 close to the values given in the literature [42-43]

Results [11] on the successful reaction synthesis of nanostructured intermetallic $Ni_{50}Al_{50}$ starting from elemental nanopowders. The observed difference in particle size calculated by XRD and observed by SEM may be due to the different clustering of the nanoparticles in agreement with others results [38]. At first, the primary NiAl phases would precipitate from the Ni-rich liquid. As the temperature decreases below 1395 °C, the peritectic reaction L + NiAl -----> Ni3Al + Al0.42Ni0.58 can occurs. Consequently, XRD analysis confirms the formation of Ni3AI + Al0.42Ni0.58 + NiAl microstructure in the as-cast-alloy in the slow cooling rate of the casting process Fig.7b. On the contrary, there is only one cubic NiAl-phase existed in the fast cooling rate with our process Fig. 7a.

Ni-rich alloys are characterized by lower porosity, resulting in an increase in lattice parameter of Ni3Al phase involving an increase in density with increasing Ni content as seen in Table 1, in agreement with other works [44-47].

CsCI

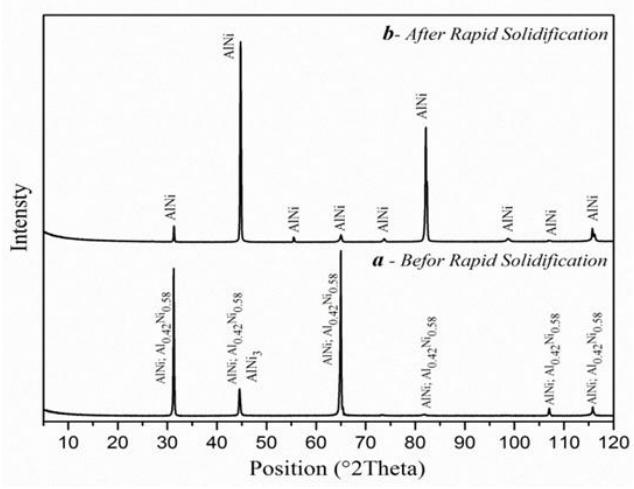

Fig 7. XRD curves of the investigated alloys in two different states; a) Ni50Al50 alloy conventionally cast ingot synthesized by induction furnace All the peaks sample are indexed as NiAl, Ni0.58Al0.42 and Ni3Al phases and b) XRD spectrum of the synthesized nanostructured Ni50Al50 alloy by rapidly quenched voice, all the peaks sample are indexed as only NiAl phase.

4. Conclusion

In this study, a novel synthesis method to produce nanostructured intermetallic $Ni_{50}Al_{50}$ is reported. Nanoparticles of $Ni_{50}Al_{50}$ alloy have been successfully synthesized via a new rapid solidification processing technique. Consequently, Liquid nitrogen quenching can restrain the precipitation of only cubic $Ni_{50}Al_{50}$ phase effectively. On one hand, liquid nitrogen quenching mode can inhibit the growth and agglomeration of NiAl particles. On the other hand, un-quenching mode can result also in the formation of NiAl nano-particles with large grain growth. As has been shown, rapid solidification processing, leads to the generation of fine grains in a NiAI matrix. Rapidly melt-quenched Ni–Al material demonstrates that the grain size of $Ni_{50}Al_{50}$ alloy is not uniform, some fine grains are smaller than 20 nm, and the bigger grains are about 100 nm. The average grain diameter is estimated at 74.8 nm. On the other hand, cast ingot synthesized by induction furnace exhibit a large average grain size (160-600 nm) comparatively to the rapidly quenched method. These findings have revealed a forming ability of nanocrystalline structures of this intermetallic $Ni_{50}Al_{50}$ alloy by rapid solidification undercooled in liquid nitrogen using a new quenched system. The synthesized alloy can be used to produce easily nanopowders by light milling $Ni_{50}Al_{50}$ alloy which can serve to form the matrix of the composite by sintering.

Conflict of Interest

The authors declare that they have no conflict of interest.

References

1. Miracle DB. The physical and mechanical properties of NiAl. *Acta Metall. Mater*, 1993; 41: 649–684.
2. Clarke DR, Levi CG. Materials design for the next generation thermal barrier coatings. *Annu. Rev. Mater. Res*. 2003; 33: 383–417.
3. Wood JH, Goldman EH. High-temperature materials for aerospace and industrial power, *in Superalloys II*, C.T. Sims, N.S. Stoloff, Hagel WC.(eds), John Wiley & Sons Inc., New York, 1987; 359–384.
4. Williams JC, Starke A E. Progress in structural materials for aerospace systems, *Acta Mater*, 2003, 51(19):5775-5799.
5. Sun L, Simm TH, Martin TL, McAdam S, Galvin DR, Perkins KM, Bagot PAJ Moody MP, Ooi SW, Hill P, Rawson MJ, Bhadeshia HKDH. A novel, ultra-high strength maraging steel with balanced ductility and creep resistance achieved by nanoscale b-NiAl and Laves phase precipitates, *Acta Materialia*, 2018; 1491: 285-301.

6. Bochenek K, Basista M, Advances in processing of NiAl intermetallic alloys and composites for high temperature aerosapce applications. *Progress in Aerospace Sciences*, 2015; 79:136-146.
7. Barett CA. Effect of 0.1 at.% Zirconium on the Cyclic Oxidation Resistance of b- NiAl. *Oxid. Met*, 1988, 30: 361-390.
8. Miracle DB, Dariola R. *Intermetallic Compounds, Practice*, J.H. Westbrook, R.L. Fleischer, Ed., Wiley, New York, 1995; 2:55-74.
9. Cui HZ, Ma L, Cao LL, Teng FL, Cui N. Effect of NiAl content on phases and microstructures of TiC-TiB2-NiAl composites fabricated by reaction synthesis. *Trans. Nonferr. Met. Soc. China* 2014; 24: 346–353.
10. Pettit FS. Oxidation mechanisms for nickel-aluminum alloys at temperatures between 900◦ and 1300◦C. *Trans. Metall. Soc. AIME* 1967; 239:1296–1305.
11. Jia Q, Li D, Li S, Zhang Z, Zhang N. High-Temperature Oxidation Resistance of NiAl Intermetallic Formed In Situ by Thermal Spraying. *Coatings Journal*, 2018; 292:1-16.
12. Zhang Y, Wang H, Zhang F, Lu X, Zhang Y, Zhou Q. Growth kinetics and grain refinement mechanisms in an undercooled melt of a CoSi intermetallic compound. *Journal of Alloys and Compounds*. 2019; 781: 13-25.
13. Feng LC, Chen Z, Fan Y, Zhang JY, Shen BL. Relation between undercooled solidification and solid-state grain growth accompanying dynamic segregation. *Vacuum*. 2019; 161: 71-80.
14. Perepezko JH. Kinetic process in undercooled melts. *Materials Science and Engineering*. 1997; A226-228: 374-382.
15. Perepezko J H. Solidification of highly supercooled liquid metals and alloys. *Journal of non-crystalline Solids*. 1993; 156-158: 463-472.
16. Urritia A, Tumminello S, Arico SF, Sommadossi S. Characterization of Al-Ni intermetallics around 30-60 at% for TLPB application. Calphad, 44, 108-113.
17. Xu Y, Kameoka S, Kishida K, M Demura A, Tsai P, Xu Y, Hirano T. Catalytic properties of Ni3Al intermetallics for methanol decomposition. *Mater. Trans*. 2004; 45: 3177-3179.
18. Xu Y, Yang J, Demura M. Toshiyuki Hirano, Yoshitaka Matsushita, Masahiko Tanaka Yoshio Katsuya, Catalytic performance of Ni–Al nanoparticles fabricated by arc plasma evaporation for methanol decomposition. *International Journal of hydrogen Energy*. 2014; 39- 2522: 13156-13163.
19. Wen C, et al. Processing of fine-grained aluminum foam by spark plasma sintering. *Journal of Materials Science Letters*.2003; 22: 1407−1409.
20. Ashby MF, Evans AG, Fleck NA, Gibson LJ, Hutchinson JW, Wadley HNG. Metal Foams: A Design Guide, Butterworth-Heinemann Publ. *Elsevier*. 2000.
21. Hull MS, Quadros ME, Born R, Provo J, Vinod K, Lohani V, Mahajan RL. Sustainable Nanotechnology: A regional Perspective. *Nanotechnology Environmental Health and Safety*. 2014; 395-424.
22. Santos MAF, Lobo IP, da Cruz RS. Synthesis and characterization of novel ZrO2-SiO2 mixed oxides. *Mater. Res*. 2014; 17: 700–707.
23. Fidelus JD, Lojkowski W, Millers D, Grigorjeva L, Smits K, Piticescu RR. Zirconia based nanomaterials for oxygen sensors–generation, characterisation and optical properties. *Solid State Phenomena*. 2007, 128: 141–150.
24. Pabi RJ, Murty BS. Mechanism of mechanical alloying NiAl and Cu-Zn systems materials. *Science and Engineering*. 1996; A 214: 146-152.
25. Gogebakam M, Uzun O, Karaashan T, Keskin M, Rapidly solidified Al-6.5wt%Ni Alloy. *Journal of Materials Processing Technology*. 2003; 142: 87-92.
26. Jayakumar S, Ananthapadmanabhan PV, Perumal K, Thiyagarajan TK, Mishra SC, Su LT, Tok AIY, Guo J. Characterization of nano-crystalline ZrO2 synthesized via reactive plasma processing. *Materials Science and Engineering: B*. 2011; 176(12): 894-899.
27. Thompson RJ, Zhao JC, Hemker KJ. Effect of ternary elements on a martensitic transformation in βNiAl, *J. Intermetallics*. 2010; 18: 796-802.
28. Colin J, Serna S, Campillo B, Flores O, Juarez-Islas J. Microstructural and lattice parameter study of as cast and rapidly solidified NiAl intermetallic alloys with Cu additions. *J. Intermetallics*. 2008; 16: 487-853.
29. Ozdemir O, Zeytin S, Bindal C. A study on NiAl produced by pressure assisted combustion synthesis. *Vacuum*. 2010; 84:430-437.
30. Bellezza F, Nocchetti M, Posati T, Giovagnoli S, Cipiciani A. Synthesis of colloidal dispersions of NiAl, ZnAl, NiCr, ZnCr, NiFe and MgFe hydrotalcite-like nanoparticles. *Journal of Colloid and Interface Science*. 2012; 376 (1): 20-27
31. Jorgensen DJ, Michael S, Pollock TM. Femtosecond laser ablation and nanoparticles formation in intermettalic NiAl. *Applied Surface Science*. 2015; 353: 700-707.
32. Saidi D, Zaid B, Boutarfaia S, Hadji S, Souami N, Bibérian JP. Formation of zirconium and nickel oxide nanoparticles via oxidation of quenched melted Ni-Zr alloys. *Ceramics International*. 2012; 38: 6957–6961.
33. Herlach D M, Galenko P. Rapid solidification: in situ diagnostics and theoretical modelling. *Mater. Sci. Eng. A*. 2007; 34-41: 449-451.
34. Herlach DM, Eckler K, Karma A, Schwarz M. Grain refinement through fragmentation of dendrites in undercooled melts. *Mater. Sci. Eng. A*. 2001, 20-25: 304-306.

35. Huang W, Chang YA. A thermodynamic analysis of NiAl system. *Intermetallics*. 1998, 6: 487-498.
36. Suryanarayana C, Ivanov E. Mechanochemical synthesis of nanocrystallinemetal powders. *Advances in Powder Metallurgy*. 2013, 42-68
37. Enami K, Nenno S, Shimizu K. Crystal Structure and Internal Twins of the Ni-36.8 at% Al Martensite. *Transactions of the Japan Institute of Metals*. 1973, 14(2): 161–165.
38. Ragupathi C, Vijaya JJ, Surendhar P, Kennedy LJ. Comparative investigation of nickel aluminate (NiAl2O4) nano and microstructures for the structural, optical and catalytic properties. *Polyhedron*. 2014, 72: 1–7.
39. Sun Y, Lin P, Yuan SJ. A novel method for fabricating NiAl alloy sheet using laminated Ni/Al foils. *Mater. Sci. Eng. A.* 2019, 754: 3428-436.
40. Ozdemir O, Zeytin S, Bindal C. Characterization of two-phase nickel aluminides produced by pressure-assisted combustion synthesis. *Vacuum*. 2008, 82: 311–315.
41. Povarova KB, Skachkov OA. Preparation, Structure, and Properties of Ni3Al and NiAl Light Powder Alloys for Aerospace. *Materials Science Forum*. 2007; 534-536: 1585-1588.
42. Fragea N, Kalabukhova S, Wagnera A, Zaretskyb EB. High temperature dynamic response of SPS-processed Ni3Al., *Intermetallics*.2018; 102: 26-33
43. Shevtsova L, Mali V, Bataev A, Anisimov A, Dudina D. Microstructure and mechanical properties of materials obtained by spark plasma sintering of Ni3Al–Ni powder mixtures. *Materials Science & Engineering* A. 2020; 773: 138882.
44. Schryvers D, Ma Y, Toth L, Tanner L. Electron microscopy study of the formation of Ni5Al3 in a Ni62.5Al37.5 B2 alloy—I. Precipitation and growth. *Acta Metallurgica et Materialia*. 1995; 43: 4045-4056.
45. Schryvers D, Ma Y, Toth L, Tanner L. Electron microscopy study of the formation of Ni5Al3 in a Ni62.5Al37.5 B2 alloy—II. Plate crystallography. *Acta Metallurgica et Materialia*. 1995; 43: 4057-4065.
46. Schryvers D, Moritz DH. Austenite and martensite microstructures in splat-cooled NiAl. *Intermetallics*. 1998; 6: 427-436.
47. Zhang ZX, Jiang H, Russell AM, Skrotzki W, Müller E, Schneider R. Microstructural evolution and phase transformation in the liquid-solid Al/Ni diffusion couple. *Philosophical Magazine*. 2019; 99:1103-1120.

Recommended Citation

Khenioui Y, Saidi D, Zaid B, Sadouki M, Souami N, Rahal B. Phase formation and structure in rapidly quenched $Ni_{50}Al_{50}$ alloy. *Alger. J. Eng. Technol. 2023*, 08(2):220-227. https:/dx.doi.org/10.57056/ajet.v8i2.127